PROCEEDINGS OF SPIE

SPIEDigitalLibrary.org/conference-proceedings-of-spie

TSPM f/5 Nasmyth configuration

Joel Herrera Vázquez, María Herlinda Pedrayes, Gerardo Sierra Díaz, Michael G. Richer, J. Jesús González G., et al.

Joel Herrera Vázquez, María Herlinda Pedrayes, Gerardo Sierra Díaz, Michael G. Richer, J. Jesús González G., William H. Lee Alardin, Carlos Tejada de Vargas, "TSPM f/5 Nasmyth configuration ," Proc. SPIE 10700, Ground-based and Airborne Telescopes VII, 107003T (6 July 2018); doi: 10.1117/12.2313030

SPIE.

Event: SPIE Astronomical Telescopes + Instrumentation, 2018, Austin, Texas, United States

TSPM f/5 Nasmyth configuration

Joel Herrera Vázquez*[a], María Herlinda Pedrayes[a], Gerardo Sierra Díaz [a], Michael G. Richer [a], J. Jesús González G [b], William H. Lee Alardin[b], Carlos Tejada de Vargas [a]
[a] Instituto de Astronomía – Universidad Nacional Autónoma de México, Carretera Tijuana-Ensenada km107, Playitas, Ensenada Baja California México CP 22860. [b] Instituto de Astronomía – Universidad Nacional Autónoma de México Av. Universidad 3000, Circuito Exterior S/N Delegación Coyoacán, C.P. 04510. Ciudad Universitaria, Ciudad de México, México.

ABSTRACT

We present the optical design, the error budget, the differential distortion budget and the baffle design of the Telescopio San Pedro Mártir f/5 Nasmyth configuration. The TSPM in its Cassegrain configuration will be assembled around a closed design (converted MMT/Magellan telescope) with most of its optical parts already manufactured. To anticipate for future possible upgrades, the project includes the design of an extreme f/5 Nasmyth configuration. Our optical design demonstrates the feasibility of the configuration, closes the interfaces to the telescope, provides a full picture of the expected performance, and identifies the critical points involved in the configuration.
Keywords: Telecentric, Nasmyth, TSPM, Error budget.

1. INTRODUCTION

The TSPM project consists in the construction of a 6.5m telescope which will be installed at the Observatorio Astronómico Nacional on the Sierra San Pedro Mártir in northern Baja California, Mexico [1]. TSPM on its Cassegrain configuration will be assembled around a closed design (converted MMT/Magellan telescope) with most of its optical parts already manufactured, the primary mirror was casted by the Arizona university (AU) and the collaboration with Harvard university includes some of the Cassegrain (Day one) instrumentation and the Wide field corrector (WFC) for imaging and spectroscopy for 0.5º and 1º respectively. To guaranty the feasibility of future possible upgrades to admit heavier and biggest instruments, the project has considered the design of extreme Nasmyth configuration that requires the development of a new secondary mirror (M2), tertiary mirror (M3). Since the nominal telescope has strong field curvature as could be expected for this design, also requires (WFC) lens.

1.1 High level requirements (HLR)

The optical design was made taking into account the high level requirements:

- FOV 1.0º in diameter in wide field (Spectroscopic Mode) and FOV 0.5° (goal: 1°) in diameter in wide field (Imaging Mode).
- A telecentric FOV should be provided for the spectroscopy mode and a flat image plane for the imaging mode.
- The plate scale (PE) of the f/5 Nasmyth focal stations shall be 170μm/” at the optical axis.
- The secondary mirror shall be designed and optimized only for this configuration and associated to that.
- The delivered image quality at the imaging mode shall allow a 12% degradation of the 10th-percentile seeing reported by Skidmore et al. (2009, PASP, 121, 1151). The reported 10th-percentile seeing is 0.5” at 5000Å. The tolerances for active optics and telescope alignment for imaging mode shall be derived from this budget and shall also be applied to the spectroscopy mode.
- M3 shall be the same for f/5 and a possible f/11 Nasmyth configuration and shall be optimized for f/5 Nasmyth.
- Wavelength range from 0.35μm to 1.0μm.
- The maximum differential image distortion at the edge of the FOV shall be a 2.5% of the nominal plate scale (i.e., a maximum displacement of ± 0.15") for the f/5 Nasmyth FOV.
- A fully baffled system in the f/5 Nasmyth 1ºFOV shall be provided.

*joel@asto.unam.mx; phone 011 52 646 174 4580 ext. 426; fax 011 52 646 174 4607; http://www.astrosen.unam.mx

Ground-based and Airborne Telescopes VII, edited by Heather K. Marshall, Jason Spyromilio, Proc. of SPIE Vol. 10700, 107003T · © 2018 SPIE
CCC code: 0277-786X/18/$18 · doi: 10.1117/12.2313030

2. OPTICAL DESIGN

The common elements shared between the Cassegrain and Nasmyth are the Primary Mirror (M1) and the atmospheric dispersion corrector (ADC). The optical design is limited by the fact that the primary mirror is a parabola, which limits the family of possible solutions for secondary mirror (M2) and thus requires to use a WFC. Table 1 shows the specifications of the M1 and M2.

Table 1. M1 and M2 specification.

Element	R(m)	Diameter(m)	K
M1	-16.25	6.5	-1
M2	-6.128	2106	-2.5834

In the case of the tertiary mirror, the mayor and minor axis of the ellipse (a= 1440mm, b=2000mm) are sufficient to cover all the required field (1°) and a little more to avoid common polishing problems and on the other hand, avoid vignetting. In Figure 1. Can be seen the bare telescope.

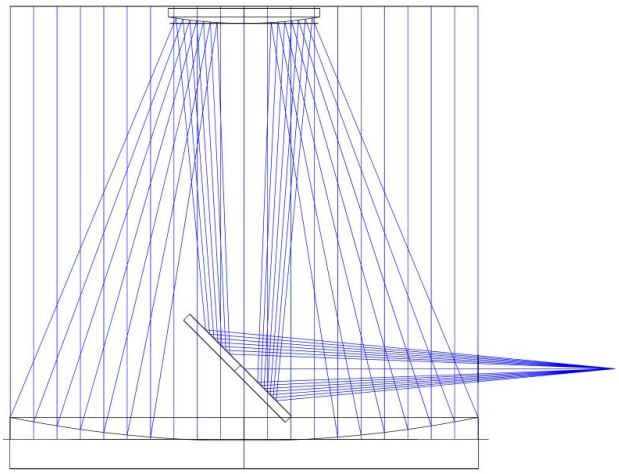

Figure 1. Bare Nasmyth optical layout Since the Nasmyth configuration is based on a classic Cassegrain system, the bare telescope produces geometrically perfect on-axis images that degrade rapidly as we move away from the optical axis. The foregoing forces us to use a WFC.

The size of M2 is governed by the imposed field, plate scale and the need to laterally move the image plane away from the area of M1. Another reason to separate the image plane is to exceed the metal structure of the altitude axis and M1 cell thickness [3]. It is important to keep in mind the ratio of collected area. In
Table 2 can be seen the impact of the M2 size in the ability to collect light.

Table 2. Effective light collector area, light loss is inevitable, and we must bear in mind that we are working with an extreme configuration.

Element	Area(m^2)
Primary	33.21
Secondary	3.48
Total used area	29.72
M1 Percent non-overshadowed	89.5%

Is important to mention that for this document, for simplicity will be considered that the images resemble a Gaussian distribution, then will be evaluated like so.

2.1 Spectroscopic Mode

The wide field corrector for spectroscopic mode includes four lenses and provides a telecentric, curved, and well-corrected image plane on a circular 1.0º FOV. It uses the existing ADC provided by the Cassegrain configuration

Table 3. Wide field Spectroscopic Configuration. The image plane is telecentric, a feature that gives advantages when using instruments with optical fibers.

Element	ROC(mm)	Thickness(mm)	Material	Diameter(mm)	Conic(K)
Primary	-16255.3	-5785.63	MIRROR	6502.4	-1.0000
Secondary	-6128.43	5785.63	MIRROR	2106.0	-2.5834
		-1000.00		1250.2	
Tertiary	Flat	-3252.00	MIRROR	1989.9	
		-176.48		921.8	
Corrector lens 1	-1774.1	-63.00	SILICASCHOTT	870.0	
	-1188.9	-90.00		850.0	
Corrector lens 2	Flat	-67.50	SILICASCHOTT	866.2	
	2445.40	-473.98		865.5	
ADC Prism 1		-25.40	S-FSL5Y	748.9	
		-0.13	CAF2SCHOTT	748.9	
ADC Prism 2		-15.24	PBL6Y	748.9	
		-25.71		748.9	
ADC Prism 3		-15.24	PBL6Y	748.9	
		-0.13	CAF2SCHOTT	748.9	
ADC Prism 4		-25.40	S-FSL5Y	748.9	
		-373.58		750.5	
Corrector lens 3	1353.84	-40.00	SILICASCHOTT	685.0	
		-293.56		687.1	
Corrector lens 4	-2469.83	-60.00	SILICASCHOTT	700.1	
	3201.53	-204.00		698.8	
Image Plane	4046.09			617.9	-71.135

The ADC is compound by 4 prisms cemented in pairs, each pair of prisms rotates coordinately in opposite directions depending of the air mass. Table 3. present the spectroscopic configuration. The Figure 2. *WFC. Spectroscopic mode, the lenses L1, L2, L3 and L4 are composed of fused silica which guarantees the transmission in the spectral range 0.35μm to 1.0μm.* shows the wide field corrector configured for spectroscopy.

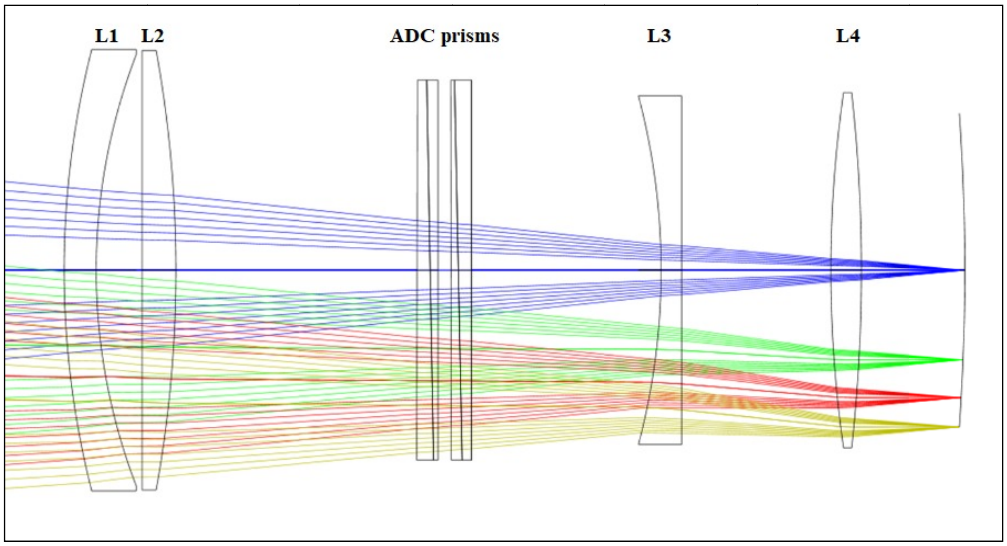

Figure 2. WFC. Spectroscopic mode, the lenses L1, L2, L3 and L4 are composed of fused silica which guarantees the transmission in the spectral range 0.35µm to 1.0µm.

Figure 3 shows the spot diagrams for the optical axis, the middle and the edge of the FOV. The circle that encloses the spots indicates the average plate scale 170µm/", in this figure we also can notice the degradation increases with the field.

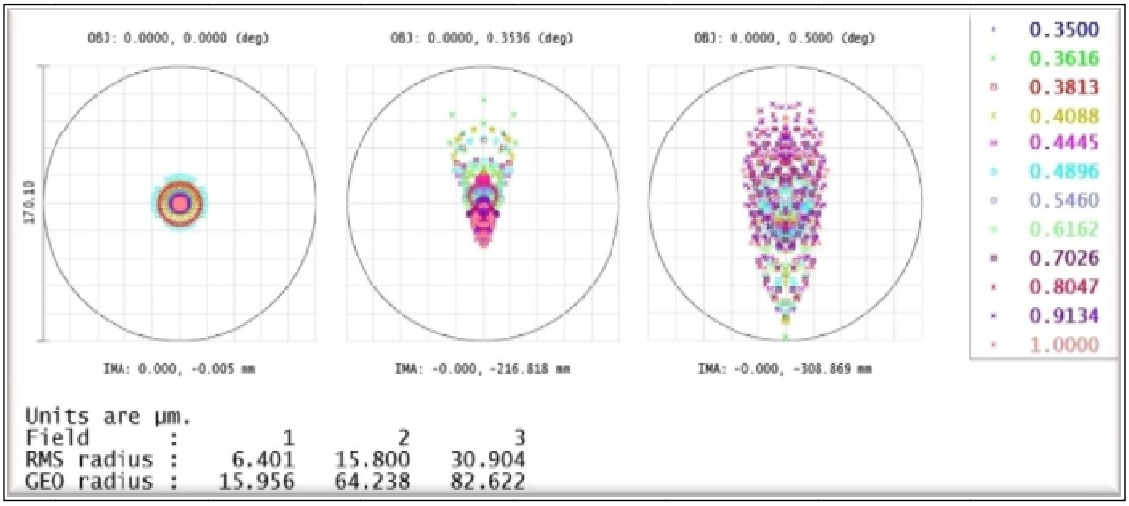

Figure 3. Spot diagram. Spectroscopic mode, the circle that encloses the spots indicates the average plate scale 170µm/".

A different way to visualize the image quality through the field is through the encircled energy plot shown in Figure 4, where each color corresponds to the encircled energy calculated polychromatically for each field.

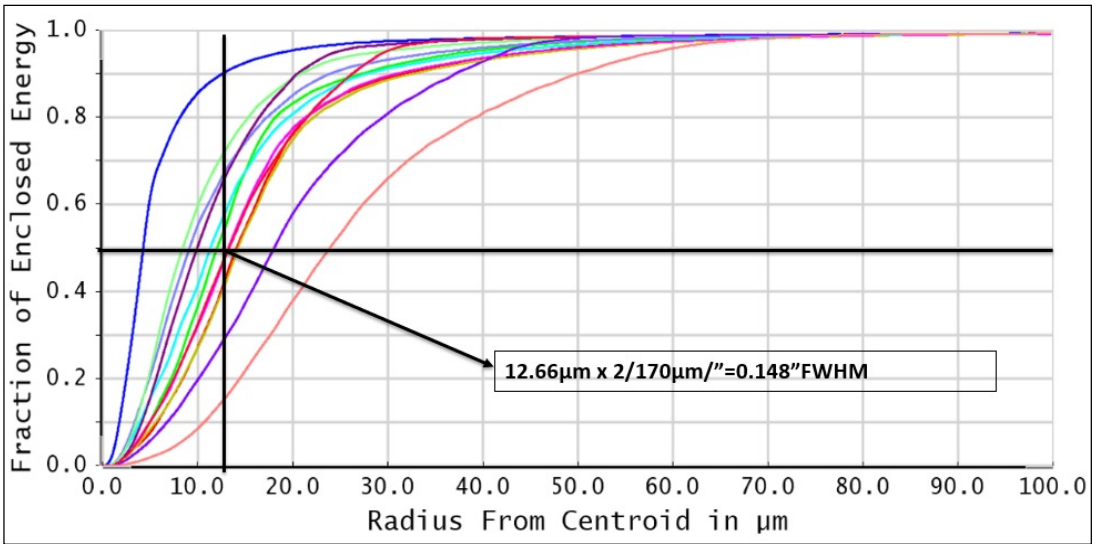

Figure 4. 2D Encircled energy (EE), 50%, each color corresponds to a field in the image plane, the widest curve (pink) represents the edge of the field, and the thinness (blue) corresponds to the optical axis.

It is very important to mention the characteristics of the image plane, since the curvature and distortion have an impact on the instrumentation placed in this focal station. Figure 1. shows the field curvature and the sagitta in the edge of the FOV (Left). The central image shows the field curvature measured on the curved image plane with the intention of evidencing the presence of chromatic aberration, and in the right side the field distortion.

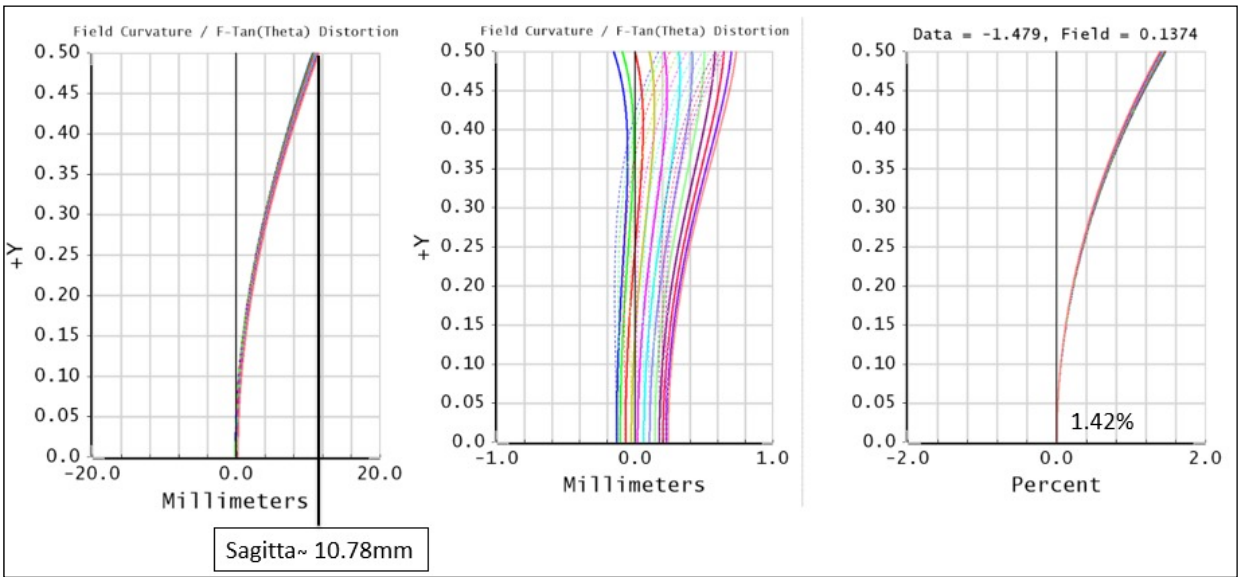

Figure 5. Field curvature and distortion. (Left) Field curvature. (Center) Field curvature on the curved image plane. (Right) Field distortion. Spectroscopic mode.

Regarding the vignetting, it is important to mention that the system vignetting is not caused by the corrector in the spectroscopic configuration, then the only vignetting is due by the obstruction that the secondary mirror generates, without considering the baffling.

2.2 Imaging Mode

The optical design for the wide field corrector for imaging mode includes four lenses and provides a flat, and well-corrected image plane on a circular 1.0º FOV (Table 4).

Table 4. Imaging configuration. The optical design provides 1º FOV and flat image plane.

Comment	ROC(mm)	Thickness(mm)	Material	Diameter(mm)	Conic(K)
Primary	-16255.30	-5784.22	MIRROR	6502	-1.00
Secondary	-6128.43	5784.22	MIRROR	2106	-2.58
		-1000.00		1254	
Tertiary	Flat	0.00	MIRROR	1994	
		-3526.73		926	
		-274.73		926	
Corrector lens 1	-1774.10	-63.00	SILICASCHOTT	870	
	-1188.90	-219.16		850	
Corrector lens 2		-67.50	SILICASCHOTT	853	
	2445.40	-1036.00		852	
Corrector lens 5	806.20	-55.00	N-BK7	655	-2.02
	2205.30	-22.86		666	
Corrector lens 6	-660.50	-55.00	SILICASCHOTT	670	
	-691.10	-169.78		655	
Image Plane				656	

The wide field corrector configured in the imaging mode Figure 6, the imaging mode doesn't use the ADC but uses the first two lenses of the corrector from the spectroscopic mode. These two lenses are relocated in a different place and the last two lenses are replaced by a new pair (L5 and L6).

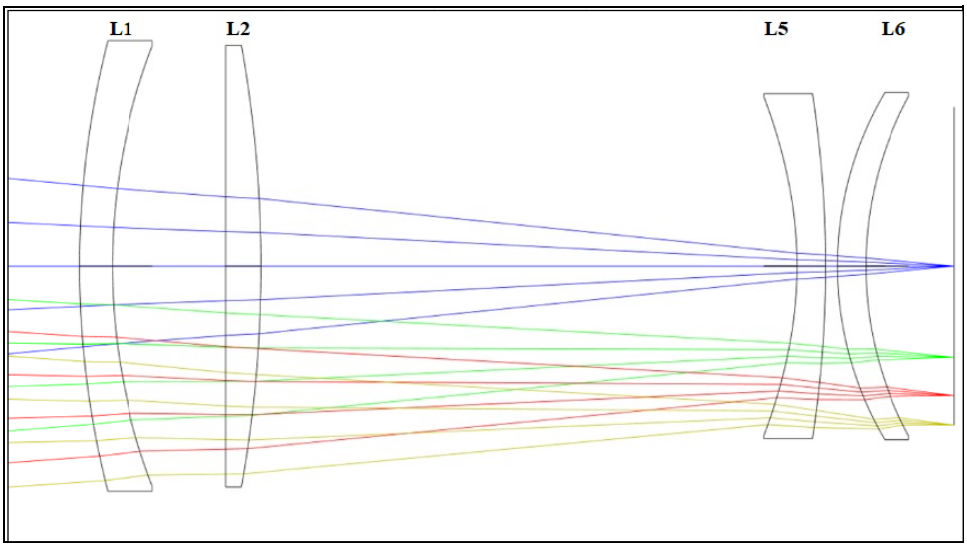

Figure 6. WFC. Imaging mode. Lenses L1, L2 are the same than for spectroscopic mode and L3 are also composed of fused silica and L4 is made on N-BK7 to keep the transmission in the spectral range (0.35μm to 1.0μm)

Figure 7 shows the spot diagrams for the optical axis, the middle and the edge of the FOV, the circle that encloses the spots indicates the average plate scale 169µm/”, in this figure we also can notice that the degradation increases with the field, however, the degradation is less than that presented in the spectroscopic mode.

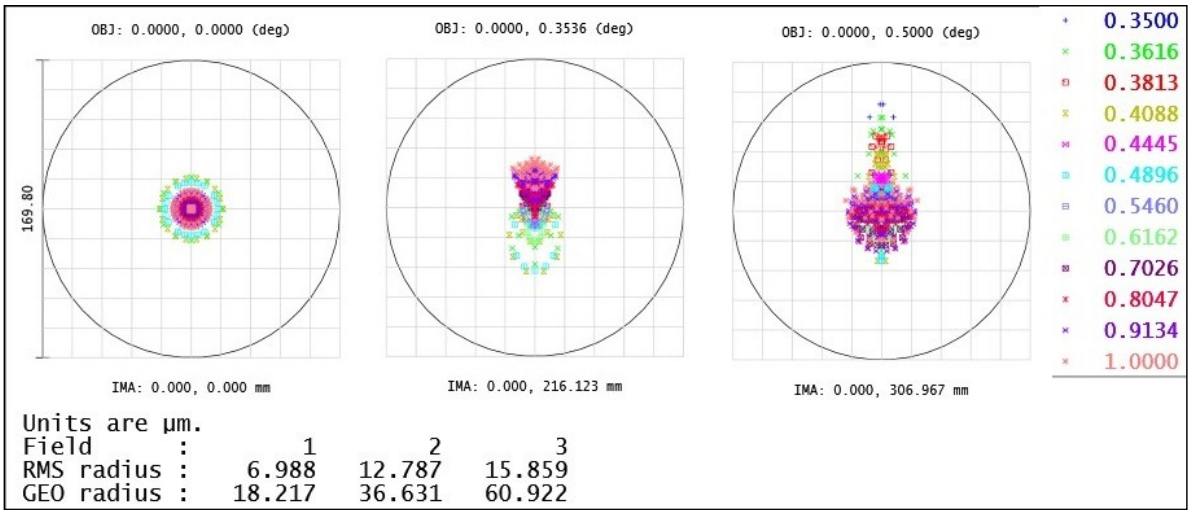

Figure 7. Average image quality 0.091” FWHM. The circle that encloses the spots indicates the average PE 169.8µm/”.

In the same way than in the previous section, Figure 8 shows a different point of view to visualize the image quality over the field.

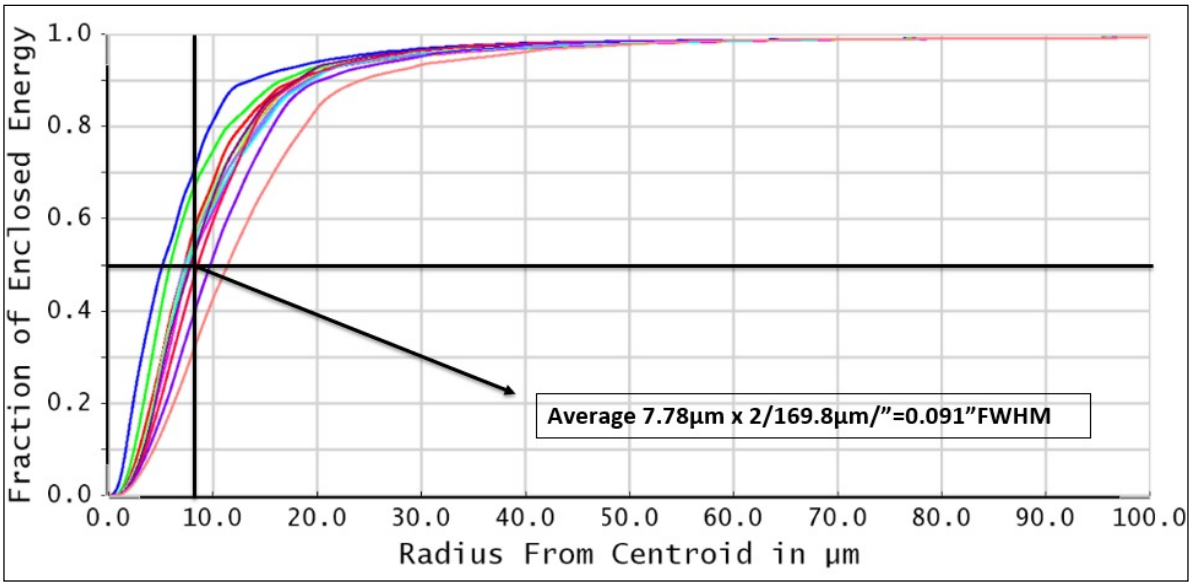

Figure 8. 2D Encircled energy, Imaging mode. The encircled energy plot shows polychromatically, each field is represented by a color.

The image plane flatness can be seen in Figure 6 (left), and the field distortion on the (right).

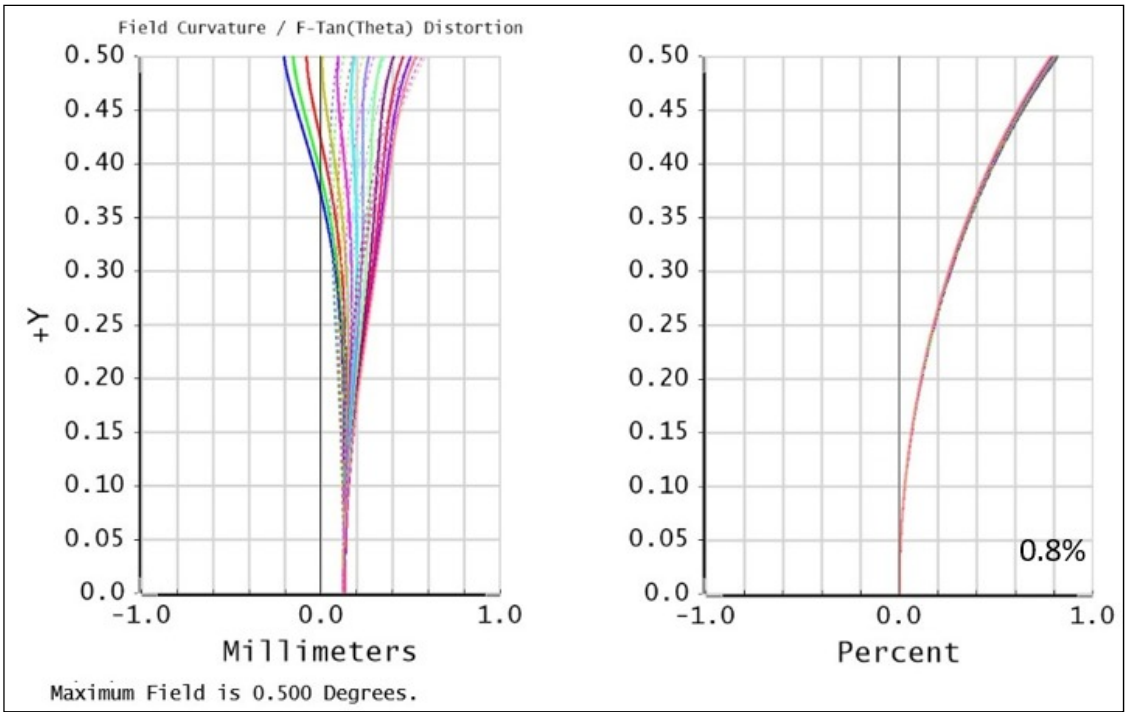

Figure 9. Imaging mode image plane characteristics in 1º FOV. Field curvature (Left), colors represent different wavelength. (Right) field distortion.

3. ERROR BUDGET

The error budget is presented (Table 8) regarding optics performance, different budget pieces are allocated to contain the main error sources that can be modeled with a reasonable effort. Nevertheless, it could be expected some further degradation due to unpredictable sources, such as windshake of the telescope structure or wave front sensor closed loop sensitivity that will set the ultimate correction level during active optics operation. All the system tolerances used for the error budget in Spectroscopic mode are the same as the used in the imaging mode and are like those used in Cassegrain configuration, providing a good level of confidence in the future upgrades.

The contributions to the error budget in both operation modes are presented in Figure 10, where the parameters considered in each contribution can be seen. Some contributions were taken directly from the documentation of the existing elements, such as the structure function that AU uses for M1.

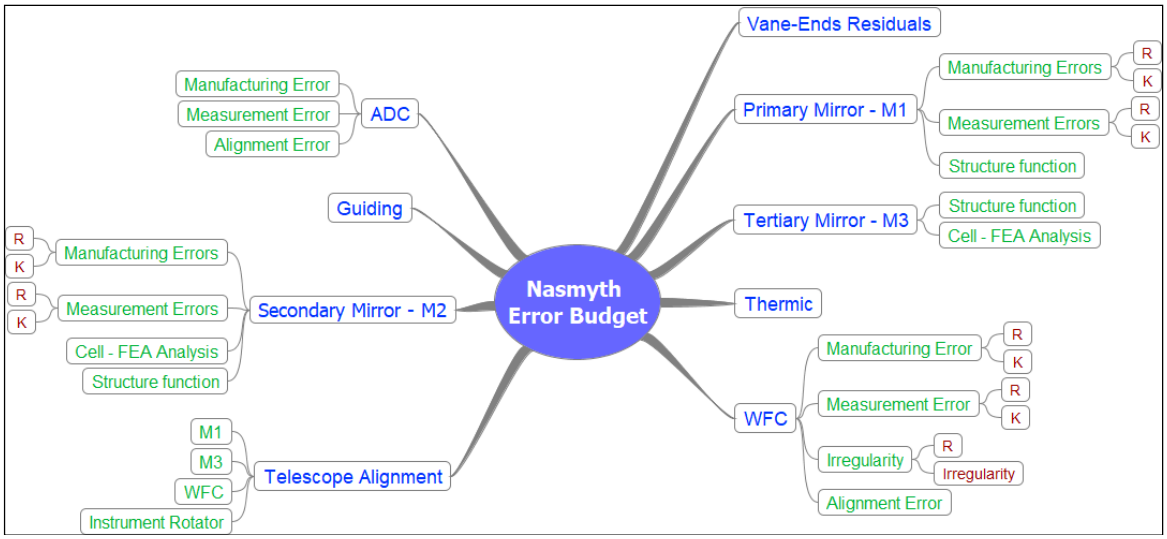

Figure 10. Error budget organization. tolerances analysis was carried out, using as compensator the position and orientation of M2 that is planned, it will be manipulated by Vane-Ends.

The tolerances and contributions has been calculated with Zemax® using Monte Carlo analysis taken in a normal distribution (Gaussian probability within the tolerance range), the optical quality of the nominal design was measured in terms of FWHM. The FOV was sampled with 12 fields representing equal areas and 12 wavelengths, the merit function was built to evaluate directly the radius to the 50% EE in radially integrated and to process the average, in that way the tolerance analysis provides directly the FWHM in arc seconds (“).

The only difference done in the estimation of the image quality for spectroscopic and imaging mode is that for spectroscopic mode, The EE has been considered monochromatically (All wavelength spots at the same time, affected by the color shift) and monochromatically for imaging (individual wavelength on the EE calculus).

3.1 M1 errors

For the M1 related uncertainties have been considered the low order ***Manufacturing errors***, (radius of curvature and the conic constant). Manufacturing tolerances provided by UA are (-16255.3 ± 3mm) for ROC and (-1 ± 0.0002) for K. Once M1 is manufactured, the as built ROC and K values are feedback in the design. We allow moving the M2 position and the corrector + focal distance from the nominal position. The ***Measurement errors*** of the ROC and CC cannot be compensated except with the M2 position adjustment for focusing. The uncertainties are -16255.3 ± 1mm for ROC and -1 ± 1x 10^{-4} for K. The uncertainties in the measurement were provided by UA.

The UA has specified M1 surface error ***Manufacturing Errors. High order*** (Table 5) using a structure function to specify error (polishing effects) at different spatial frequencies (from mm to meter level) and using the Kolmogorov turbulence model to obtain the structure function. So, degradation is compared to the natural seeing baseline structure function [2]. To convert the Frieds parameter to the contribution in term of the FWHM we use the equation (1)

$$FWHM = 0.98\left(\frac{\lambda}{R_0(\lambda)}\right) \quad (1)$$

Table 5: M1 summary surface quality specifications.

R_0 (Frieds, cm)	λ (nm)	Max TIS	Roughness	D
> 91 (goal 118)	500	2% (goal 1.5%)	< 20 Å	6.5 m

Notice than the total contribution for M1 high frequency errors are the sum of many different factors Table 6, from MMT error budget we got the values of these additional parameters and integrate to our error budget with our M1 Freed parameter. The values on Table 6 are not added in quadrature, they are added in terms of R_0 with $\sum R_0^{-\frac{5}{3}}$.

Table 6. M1 Hight frequency errors contributions.

Error Source	Image FWHM (´´)	R_0(cm)
Polishing/ Testing	0.11	91
Primary Support	0.072	141
Wind Forces	0.05	214
Ventilation Errors	0.05	214
Material Homogeneity	0.05	214
Reflective Coating	0.025	400
Total primary	0.184	55

3.2 M2 errors

The uncertainties are presented in Table 7. For the calculus of M2 involved contributions to the error budget, the analysis uses the same errors and uncertainties than are presented in M2 MMT and Magellan reports, understanding than the manufacturing techniques can be the same for the M2 Nasmyth. The Frieds parameter (R_0) was also adjusted.

Table 7. M2 Errors, uncertainties and compensators.

	ROC (mm)	K	Compensator
Manufacturing Errors	6128.431 ± 2 mm	-2.5834± 0.001	M2 focus position, corrector/focal plane position and back focal distance
Low order. Uncertainties	6128.431 ± 0.202 mm	-2.5834± 0.0004	M2 focus position
High order (Structure function)	R_0 (Frieds , cm) > 253 (0.04" FWHM)		No compensator

3.3 M3 errors

For the ***M3 low order errors*** has been used the curvature tolerance ± 1 fringe in the irregularity of the surface (departure from flatness in interferogram fringes) as well as a combination of ± 1 fringe of spherical + astigmatism. For the ***M3 high order errors***, the same polishing specification as for M2 has been used. As the M3 used footprint is half M2 footprint the equivalent R_0 scales to twice at the grand total budget. As the M3 used footprint is half M2 footprint the equivalent R_0 scales to twice at the grand total budget. For the error budget M2 R_0=253 cm is equivalent M3 R_0=506 cm at the pupil budget. In any case the polishing spec scales a factor 6.5 to the surface so the polishing spec will have an error of R_0=78cm or 0.02" FWHM.

3.4 M2 and M3 support contributions

The design of the M2 and M3 are honeycomb type to minimize the weight and flexions on the optical surfaces, the structural design is considering the strategy to hold the mirror in the better form possible to minimize the effect of the supports in touch with the mirrors. Unfortunately, in both cases the static support is not enough, and each mirror need an active cell. To calculate the contribution of the M2 and M3 supports to the final image quality it was performed a FEA analysis in conjunction with Zemax®, using the deformation of the optical surface including a "*grid sag element"* to the optical element.

The contribution of the M3 active cell is 0.011" FWHM, in the case of M2 the mechanical design is not complete and do not include active system, the contribution is 0.107" FWHM which is unacceptable. The error budget for the Nasmyth spectroscopic configuration (0.565" FWHM) do not fulfill the requirement of 12% in degradation from the seeing (0.5" FWHM). The error budget presents a value of 0.0505" FWHM, which is the maximum allowable to fit the error budget at least for an image configuration. The design of the active optics for M2 is in development.

3.5 WFC fabrication and alignment

For all the corrector elements fabrication, the used tolerances were ±1mm in the ROC, ±3mm in thickness, a wedge angle of ±0.0141º and an irregularity for the astigmatism and sphericity of ±1 interference fringe. For the analysis was used the axial position of M2 and the position of the image plane as compensator. For the corrector alignment the elements were separated in three sub groups that can be mechanically joint inside a main barrel, the analysis considers the misalignment of each individual element between its group and later the misalignment of the three groups inside the barrel. The alignment errors choices for the analysis (for elements and groups) were ±0.1mm for the axial position, ±0.14 for the radial position error and ±0.013º for tilts.

3.6 Thermal errors

The error budget includes two different contributions due to the temperature considering homogenous changes through the optical system. The "***Thermal compensation residual"*** is originated from moving M2 to practically recover the optical performance over the analyzed temperature (-5°C to 20°C) range is 0.0083". The ***"Thermal -0.05 deg(c)"*** is the maximum degradation on the image quality (0.037" FWHM for spectroscopy 0.0175" FWHM for imaging) over all the temperature range compensating with M2 and including an error of 0.05°C on the thermometers resolution.

Table 8. Error budget. (Left) Spectroscopic mode, (Right) Imaging mode.

ITEM	SPECTROSCOPIC	IMAGING
	FWHM (´´)	
Nominal Performance	0.148	0.0914
M1 Manufacturing, High Order With AO	0.184	0.1840
M1 Manufacturing Errors. Low Order.	0.0154	0.0143
M1 Manufacturing Error Uncertainties	0.0537	0.037
M2 Manufacturing Errors Low Order	0.0124	0.0114
M2 Manufacturing Uncertainties	0.0411	0.0189
M2 Manufacturing. High Order	0.0400	0.0400
M3 Manufacturing, Surface Irregularity, Curvature	0.0186	0.0110
M3 High Order. Structure Function	0.0200	0.0200
Corrector Fabrication	0.0400	0.0332
Corrector Alignment	0.0440	0.0124
Telescope Alignment	0.0504	0.0192
M2 Active Optics Residuals	0.0174	0.0207
Thermal-Toler	0.0082	0.0084
Thermal-0.05º (C)	0.0372	0.0175
Guiding	0.0300	0.0300
M3 Cell	0.0110	0.0110
M2 Cell	0.0505	0.0505
Seeing	0.5	0.5
Total	0.57	0.55

4. DIFFERENTIAL DISTORTION BUDGET

The TSPM focal plane distortion introduces a requirement on the alignment between the mechanical rotator axis and the optical axis. In case of failing this requirement, multi-slit spectroscopy would loss objects in slits as field rotates. The purpose of this analysis is to guarantee this requirement. A tolerance analysis was performed for all the elements that affect this parameter (alignment tolerances).

Table 9. Differential distortion budget.

ITEM	Movement (")
Nominal	0.000
Telescope Alignment	0.118
Corrector Alignment	0.199
ADC bore sight	0.110
Total	0.257

We have allocated 0.257" (Table 9) of differential shift for this budget piece (total budget for Cassegrain 0.3"). We have used Zemax® and the differential shift has been computed for two objects separated 0.5º. At this position we obtain the maximum shift within the 1º FOV, so this is the worst-case scenario. The parameters that introduce a decenter in the optical axis are tilts, decenters and lens wedges. Axial movements do not affect the results. As the field corrector is not already manufactured, making the analysis of this piece has sense in difference with Cassegrain configuration. We allocated some of the budget to the boresight of the corrector and will focus our work on the alignment of the different pieces: M1, M2, M3, WFC and Rotator interface (Table 10).

Table 10. Alignment tolerances.

	Dx (mm)	Dy (mm)	Dz (mm)	Rx (")	Ry (")
M1 in cell	± 1	± 1	-	± 30"	± 30"
WFC to cell	± 0.1	± 0.1	-	± 20"	± 20"
Rotator to cell	± 0.13	± 0.13	-	± 30"	± 30"
M2	Comp	Comp	Comp	Comp	Comp

5. COMPENSATOR RESOLUTION

The compensator considered in the error budget is M2 position and orientation, whose active optics system will be positioning M2 during the observation to compensate misalignment in the optical axis of the telescope due to gravitational structure strain and thermal changes. M2 is mounted on a vane-ends mechanism and the mechanical resolution required has been also calculated (Table 11).

Table 11. Compensator resolution (M2 active system).

Dx (mm)	Dy (mm)	Dz (mm)	Rx (“)	Ry (“)
± 0.003	± 0.003	± 0.001	± < 0.5	± < 0.5

As the system cannot provide better adjustment than the mechanism resolution, the error associated to this system has been evaluated. The Monte Carlo analysis was done with the previous tolerances and no compensation of any type. It is important to mention that the precisions included in this section are those that have been requested throughout the range

of the mechanism to guarantee the optical performance, however, it has been demanded better incremental precisions that shall apply to smaller range and a better measurement resolution.

6. BAFFLE SYSTEM

In this preliminary design the envelopes of the main baffles M1 and M2 were obtained for one-degree field, it provides minimal obstruction and prevent the arrival to the detector of any rays directly coming from the sky (Figure 11) or the telescope building. It is not a detailed design and it needs to be optimized for aspects as weight, section to the wind, paint, and stray light reflected on its surfaces. Table 12. Presents the effective area for light collection.

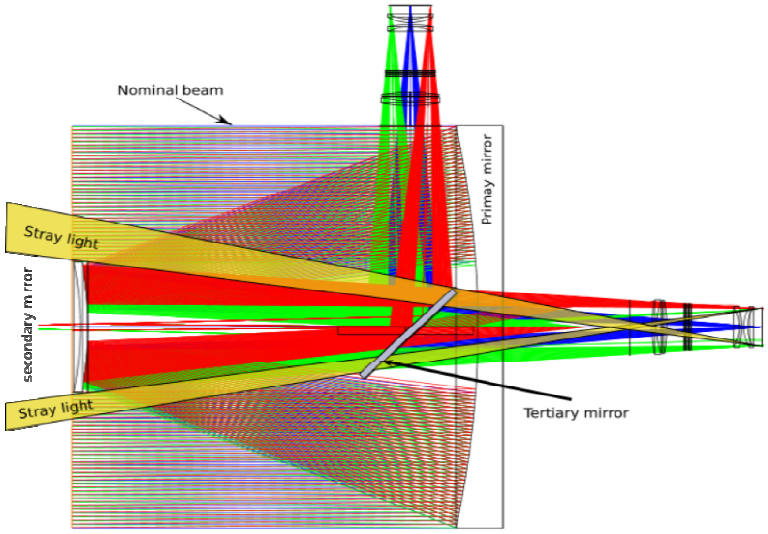

Figure 11. Sky stray light layout. The stray light is not axially symmetric because of the tilt of the tertiary mirror.

Table 12. Baffle effects on the effective area, the light loss compared to the nominal design loss (89.5%) without baffles is 3.8%.

Inner M1 clear aperture (ICA) (mm) 923.00			
Outer M1 clear aperture (OCA) (mm) 6478.00			
Area M1 (m^2)	32.96		100.0%
Area M1 OCA - Area M1 ICA (m^2)	32.29		98.0%
Area M2 (m^2)	3.48		
Area M1 not vignetted by M2 (m^2)	29.48	Useful area	89.5%
M2 baffle diameter (m)	2.45		
M2 baffle area (m^2)	4.71		
Area M1 -Area baffle M2 (m^2)	28.24	Useful area	85.7%

Figure 12 shows the general dimensions of the envelope that defines the baffle.

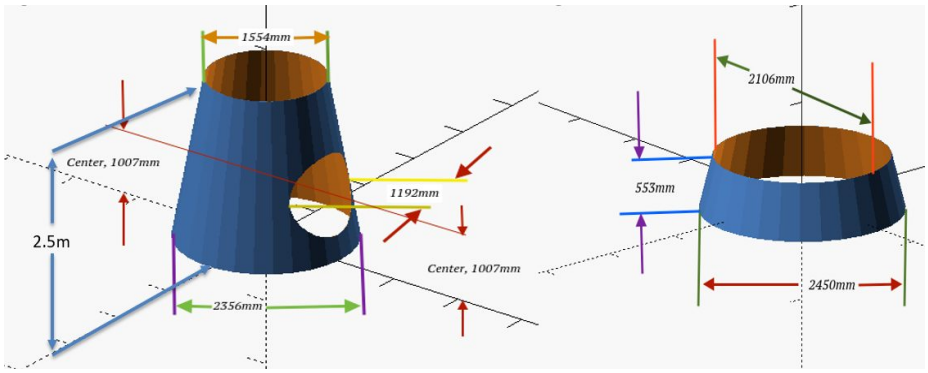

Figure 12. Baffles general dimensions. (Left) M1 baffle, (Right)M2 Baffle.

7. CONCLUSIONS

The EB for Nasmyth configuration has been done for imagining and spectroscopic mode. The design fulfills the requirements. The resulting optical design demonstrates the feasibility of the configuration, closes the interfaces to the telescope, provides a full picture of the expected performance and, in the same way, identifies the critical points involved in the configuration.

The main objective of defining the interfaces with the telescope has been fulfilled, given that the maximum envelopes of the optical elements, the masses and mainly the alignment and manufacturing tolerances were defined. The optical design has been useful to limit the design of the telescope; however, more work can be done to further optimize the spectroscopic configuration that is a little out of the HLR in terms of image quality.

The tolerances and specifications of the elements have been the same than that of the Cassegrain configuration, the only change between the Nasmyth and Cassegrain configurations is the Vane-Ends precision, but this does not represent any limitations. Current tolerances require a very precise alignment of M1 optical axis, M3, WFC and rotator to fulfill image quality also the 0.3" differential distortion requirement and leaving some space for uncertainties.

M2 and M3 supports play an important role in the image quality, the study for the M2 support is not complete and need to be optimized to fit the requirement but we think that this is not a problem because we can adopt the solution implemented by MMT and Magellan which incorporate active systems.

We propose a full baffling geometry in the 1º FOV. Two main baffles are needed, and main dimensions have been defined.

REFERENCES

[1] Jose Teran,William H. Lee,Michael G. Richer,Beatriz S. Sánchez,David Urdaibay,Derek Hill,David Adriaanse,Regina Hernandez-Limonch. “Telescopio San Pedro Mártir Observatory preliminary design and project approach”. Proceedings of SPIE - The International Society for Optical Engineering. 9906. 10.1117/12.2230767. (2016).
[2] Parks, Robert. “Specifications: Figure and finish are not enough”. Proceedings of SPIE - The International Society for Optical Engineering. 7071. 10.1117/12.798223. (2008).
[3] Jorge Uribe,Vicente, Bringas,Noe Reyes,Carlos Tovar,Aldo López,Xóchitl Caballero,César Martínez,Gengis Toledo,William Lee,Alberto Carramiñana,Jesús González,Michael Richer,Beatriz Sánchez,Diana Lucero,Rogelio Manuel,Saúl Rubio,Germán González,Obed Hernández,José Segura,Eduardo Macias,Mary García,José Lazaro,Fabián Rosales,Luis del Llano. “Mechanical conceptual design of 6.5 meter telescope: Telescopio San Pedro Mártir (TSPM)”. Proceedings of SPIE - The International Society for Optical Engineering. 9906. 10.1117/12.2232666. (2016).